

Aerofoil Tones Produced by a Streamlined Plate with Cavity

K. Schumacher, C. Doolan and R. Kelso

School of Mechanical Engineering
 University of Adelaide, Adelaide, South Australia 5005, Australia

Abstract

A streamlined plate containing a rectangular cavity on one side was found to produce aerofoil tones. In the considered chord-based Reynolds number range of 1.0×10^5 to 1.8×10^5 , cavity oscillation modes did not occur due to insufficient cavity length (being 5% of chord). The discrete tonal frequencies showed good collapse with a $U^{0.85}$ scaling, suggesting that the tonal mechanism behaves similarly to that reported for smooth aerofoils. In this instance, the results suggest that an aeroacoustic feedback loop exists between the aerofoil trailing edge, where the noise is thought to be generated, and a highly receptive point in the boundary layer located at the cavity trailing edge. A region of separation near the aerofoil trailing edge is also believed to play a role in the amplification of the tones.

Introduction

When operated at low to moderate chord-based Reynolds number (up to approximately 600,000 [1]) aerofoils may produce tonal noise. According to Arcondoulis *et al.* [2], such operation may occur, for example, in computer cooling fans, micro wind turbines and small unmanned aerial vehicles.

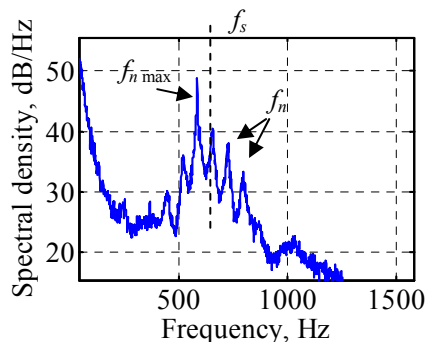


Figure 1. Typical spectral characteristics of aerofoil tonal noise, recorded for the current plate.

The noise has distinctive characteristics, often consisting of a series of approximately evenly spaced tonal frequencies (f_n) located around a broadband contribution centred about a central frequency, f_s . This behaviour has been attributed to the existence of a feedback loop of the form described by Arbey and Bataille [1]. The discrete tones are said to have a fixed total phase around the loop in order for reinforcement to occur, as specified by equation (1). Following Arbey and Bataille [1]:

1. Noise is considered to be generated by diffraction of hydrodynamic instabilities in the boundary layer at the sharp aerofoil trailing edge.
2. These acoustic waves are then considered to initiate hydrodynamic instabilities in the receptive boundary layer at some neutral stability point upstream, typically on the pressure surface.

3. Finally, these hydrodynamic waves are considered to create further acoustic waves as they pass the trailing edge, thereby closing the feedback loop.

$$\frac{f_n L}{U_c} \left(1 + \frac{U_c}{c - U} \right) = n + 1/2 \quad n = 1, 2, 3, \dots \quad (1)$$

Arbey and Bataille [1] provided two empirical relations to describe the tones. The first is a relation for the central frequency, equation (2), following the work of Paterson *et al.* [3]. The second is a relation for the discrete tonal frequencies, given by equation (3). These describe the ‘ladder structure’ found—where the overall behaviour follows a $U^{1.5}$ scaling while the individual tones form ‘rungs’ with a $U^{0.85}$ scaling. There are two empirical coefficients which are denoted K_1 and K_2 respectively. For combined NACA 0012 and NACA 0018 data these values are $K_1=0.011$ [10] and $K_2=0.85$ [1].

$$\frac{f_s}{U^{1.5}} = K_1 (Cv)^{-1/2} \quad (2)$$

$$\frac{f_n}{U^{0.85}} = (n + 1/2) \frac{K_2}{L} \quad n = 1, 2, 3, \dots \quad (3)$$

While many studies have supported the existence of a feedback loop of this form [e.g., 5,12], other studies however have disputed the feedback loop’s necessity - finding the production of tones from aerofoils *without* the presence of a loop of this form [8,9]. As of 2011, Jones and Sandberg [6] stated that the existence of a feedback loop ‘has not yet been rigorously proven’.

Nash, Lowson and McAlpine [9] explained the importance of a region of separation on the pressure surface near the aerofoil trailing edge. They proposed a new mechanism where the tones could be explained ‘purely’ by the amplification of boundary layer instabilities by the separating shear layer [9, p. 59]. The instabilities were considered to be ‘massively amplified’ in this separated region [9, p. 58].

In the current study a streamlined plate containing a cavity on the pressure side, designed for investigation of laminar cavity flow noise, was found however, at sufficiently low Reynolds number, to produce aerofoil tones. In such instances, the non-dimensional cavity length is sufficiently small that cavity oscillation modes do not occur [11]. Boundary layer velocity measurements show that an acoustic feedback loop appears to exist between the aerofoil trailing edge and the cavity trailing edge, while flow visualisation results suggest the existence of a region of separation approaching the trailing edge of the aerofoil. Thus the overall mechanism responsible for the aerofoil tones in this instance is believed to include *both* an Arbey and Bataille [1] type feedback mechanism as well as a region of separation playing a role in the amplification of the tones, following Nash *et al.* [9].

Experimental Method

Experiments were conducted in an anechoic wind tunnel facility at the University of Adelaide. The tunnel consists of an acoustically treated open jet in an anechoic chamber. A streamlined flat plate containing a rectangular cavity was placed in the jet outlet as shown in figure 2. Measurements were conducted for jet velocities in the range of $U=12$ m/s to 21 m/s. The airfoil has a chord $C=130$ mm, giving chord-based Reynolds numbers of $1.0 - 1.8 \times 10^5$. The plate thickness is 11 mm.

Velocity measurements around the plate were taken with a single-wire hot wire probe. The probe was positioned using an automatic 3D traversing system which is fixed to the chamber. Microphone measurements were taken using a B&K $\frac{1}{2}$ in. microphone (model no. 4190) located perpendicular to the trailing edge at a distance of 585 mm.

The jet has a width of 275 mm and the aerofoil's span was the same. The height of the jet is 75 mm. The true angle of attack is less than the geometric angle of attack due to deflection of the jet [3]. The geometric angle of attack used was -7° (nose-down) while the corrected angle of attack, following Brooks, Pope and Marcolini [3], was -0.9° . The front mounting point, on the chord-line and located at 15% chord measured from the aerofoil leading edge, was located 100 mm from the jet outlet and also 12 mm below the jet centreline to attempt to avoid interaction of the cavity resonance with the jet free shear layer as found by Milbank, Watkins and Kelso [7].

On the pressure side of the plate there is a 7 mm wide, spanwise cavity which is 6 mm deep and located 33 mm from the aerofoil leading edge. The cavity spans the entire plate. The cavity can be located in one of four positions, by using rectangular inserts, as shown in figure 3(a). Results are given here for cavity positions 1 and 4. Please note that the co-ordinate system origin is located at the airfoil trailing edge, however the x and y axes are aligned in the horizontal and vertical directions respectively (rather than chord-wise and normal) as described in figure 3(b).

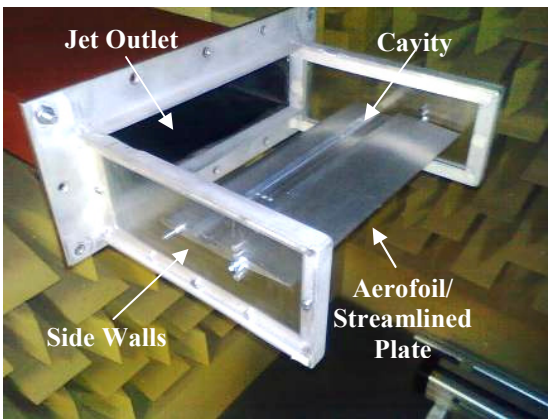


Figure 2. Photograph of experimental set-up.

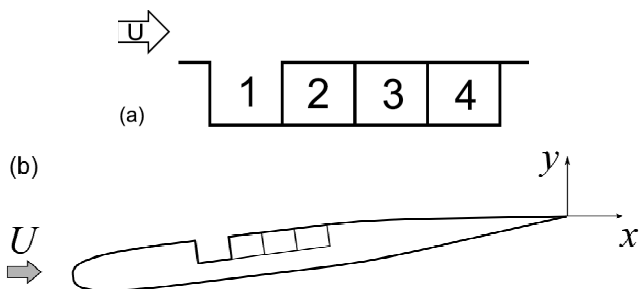


Figure 3. (a) Cavity position designations. (b) Co-ordinate system.

Characteristics of the tones and velocity scaling

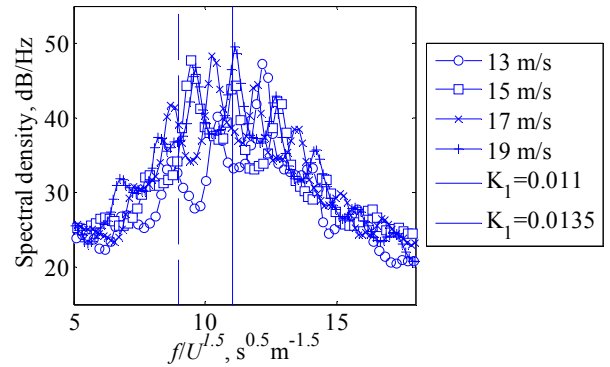


Figure 4. Frequency spectra scaled by $U^{1.5}$, for cavity position 4.

Figure 4 shows the overall behaviour of the tones. Following equation (2), the frequency spectra are scaled by $U^{1.5}$ and show good collapse with the central frequency of the broadband 'hump', $f_s/U^{1.5}$, approximately collapsing to a constant equal to $K_1(Cv)^{-1/2}$. For the current plate the empirical coefficient $K_1=0.011$, determined by Paterson *et al.* [10] for the NACA 0012 & NACA 0018 sections under-predicts the central frequency. $K_1=0.0135$ describes the behaviour better for the current plate. The empirical coefficients appear to be profile-specific.

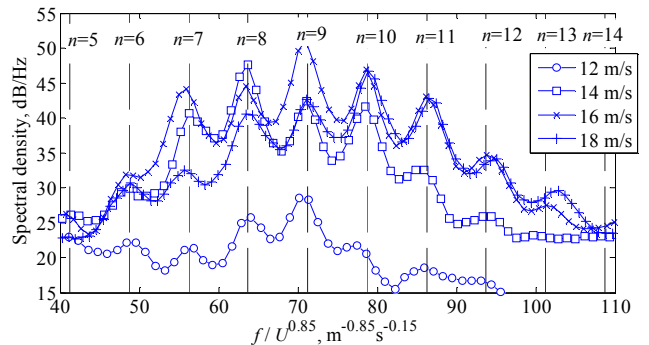


Figure 5. Frequency spectra scaled by $U^{0.85}$, for cavity position 1.

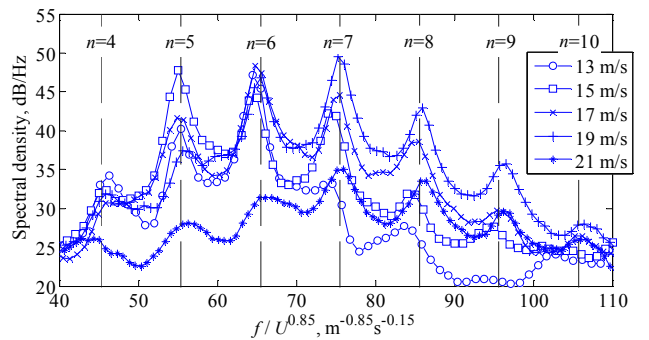


Figure 6. Frequency spectra scaled by $U^{0.85}$, for cavity position 4.

Figures 5 and 6 (for cavity positions 1, upstream, and 4, downstream, respectively) indicate that the discrete tones show good collapse when the frequency spectra are scaled by $U^{0.85}$, following equation (3). This suggests that the tonal noise mechanism behaves similarly to that reported for smooth aerofoils. The discrete values given by equation (3) are plotted as dashed vertical lines. *A posteriori* the feedback length, L , was taken to be the distance from the cavity trailing edge to the aerofoil trailing edge. It can be seen that the frequencies are spaced further apart for cavity position 4 than cavity position 1. This is consistent with the requirement of the feedback loop that $f_n \propto 1/L$. Empirical coefficients of $K_2=0.675$ for cavity position 1 and $K_2=0.695$ for cavity position 4 describe the data well, and these are lower than the value $K_2=0.85$ for the NACA 0012 [1].

Boundary layer and wake properties

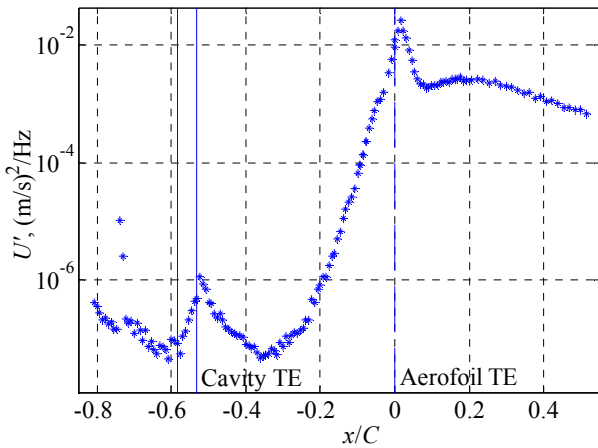


Figure 7. Power spectral density amplitude of the fluctuating velocity signal at 610 Hz (corresponding to the main aerofoil tone) for cavity position 4. Positions $x/C < 0$ were measured at a height corresponding to $u/U = 0.5 \pm 0.05$ within the boundary layer. Positions $x/C > 0$ form a horizontal line through the wake from the most downstream measurement point in the boundary layer. The solid vertical lines indicate the position of the cavity.

Figure 7 shows the spectral density of the fluctuating velocity at 610 Hz, corresponding to the main far-field aerofoil tone, for the flow configuration of $U=14$ m/s and cavity located at position 4. Local maxima are present at $x/C=-0.52$ (at the cavity trailing edge) and $x/C = 0.02$ (just downstream of the airfoil trailing edge).

The local maximum at $x/C=-0.75$ is believed to be due to slight roughness at the leading edge of the first, filled-in, cavity position, however figure 9 shows that the fluctuation detected here is acoustic and not convective in nature. The roughness has increased the detection of the acoustic wave, but convective boundary layer disturbances do not appear to be initiated here.

The velocity spectrum just downstream of the cavity trailing edge is shown in figure 8(a). There is a main peak at 520 Hz, and other peaks at 440 Hz and 610 Hz. Figure 8(b) shows the velocity spectrum just downstream of the aerofoil trailing edge. Peaks are found at 440, 520, 610 and 700 Hz. Peaks in the acoustic spectrum are at 430, 520, 610 and 700 Hz.

Figure 9 shows the phase of the velocity fluctuations at 610 Hz, relative to the reference given by the far-field microphone measurement. It shows that a convective disturbance at the aerofoil tone frequency is not detected in the boundary layer upstream of the cavity, while it is detected downstream of the cavity. Upstream of the cavity, the phase is nearly constant, varying much more slowly with position, consistent with the much longer wavelength of the acoustic wave and showing that the fluctuation detected is the acoustic component of velocity. This is consistent with the requirement of the aeroacoustic feedback loop, where the disturbance is said to be initiated at some point along the boundary layer.

From the slope of the plot, the wavelength and therefore, knowing the frequency, the convective velocity of the disturbances can be estimated. Between the cavity TE and the aerofoil TE ($-0.58 < x/C < 0$), the convective velocity is approximately $U_c = 0.40 U$. In the wake, $x/C > 0.08$, it is approximately $U_c = 0.90 U$ (based on the nominal, higher, free stream velocity upstream at the jet outlet).

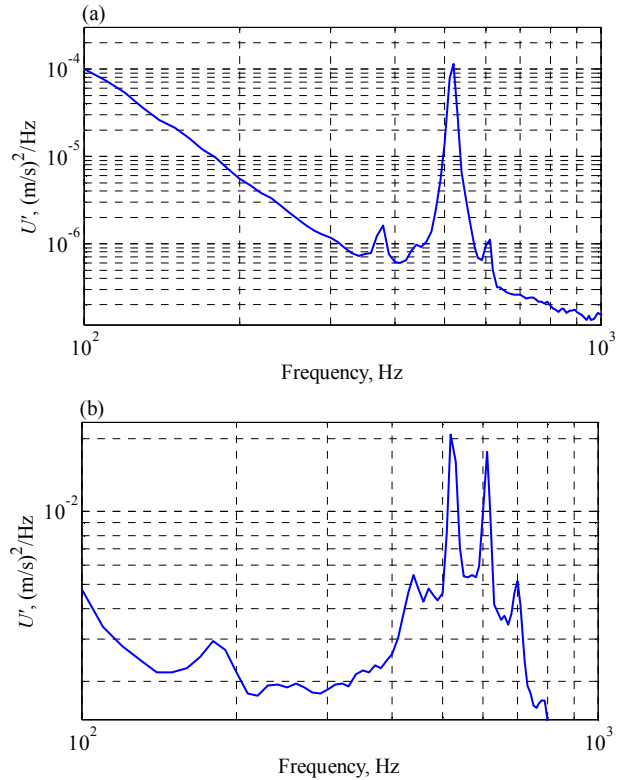


Figure 8. Spectral density of the fluctuating velocity. (a) At $x/C=-0.52$ (just downstream of the cavity trailing edge). (b) At the maximum present just downstream of the airfoil trailing edge ($x/C=0.02$). Velocity measurement heights are as per figure 7.

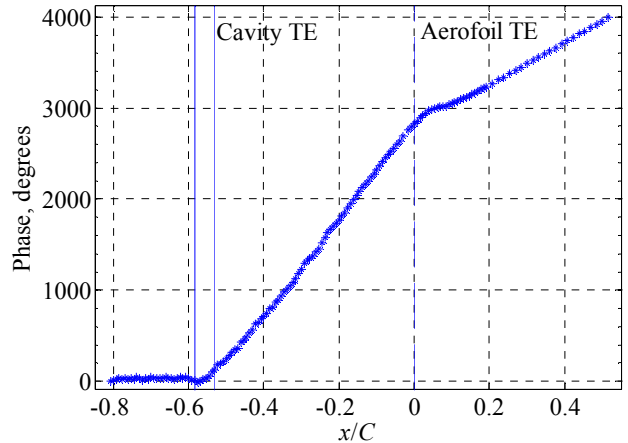


Figure 9. Phase difference at 610 Hz between the velocity measurement and far-field reference microphone. Velocity measurement heights are as per figure 7. The solid vertical lines indicate the position of the cavity.

Figure 10 shows the coherence between the velocity measurement and the far-field microphone measurement. As mentioned before, the high coherence around $x/C=-0.75$ is thought to be due to the detection of the acoustic component of velocity by the hot wire. Where the convective disturbance is detected, downstream of the cavity, there are three local maxima. The first maximum has a coherence of 0.46 and is located at $x/C=-0.52$ near the cavity trailing edge. The second has a coherence of 0.59 at $x/C=0.02$ just downstream of the aerofoil trailing edge. The third is located at $x/C=0.30$ and has a coherence of 0.59. There is a local minimum in the near-wake at $x/C=0.08$ and Moreau, Brooks & Doolan [8] attributed a similar minimum to the hot-wire disturbing the vortex formation process.

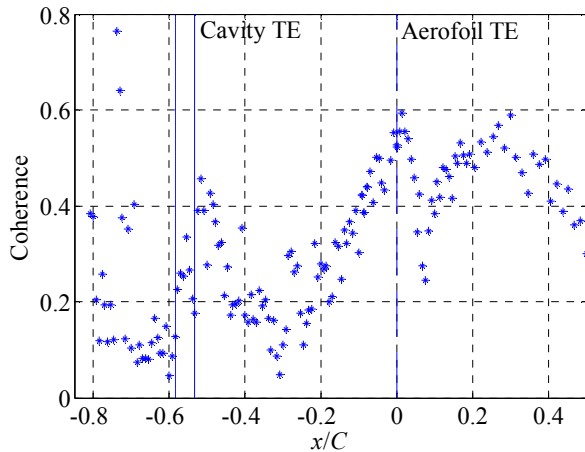


Figure 10. Coherence at 610 Hz between the velocity measurement and far-field microphone measurement. Velocity measurement heights as per figure 7. The solid vertical lines indicate the position of the cavity.

Flow visualisation

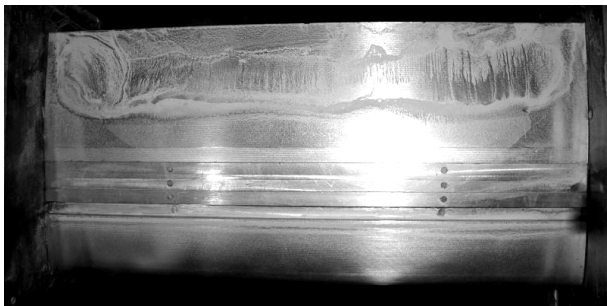


Figure 11. Surface flow visualisation of the pressure side of the aerofoil. Flow from bottom to top.

Basic surface flow visualisation was attempted. A mixture of talcum powder, ethanol and water was applied which was allowed to dry under the influence of the flow. The flow visualisation shows the existence of a region of separation along the tapered tail. Separation occurs at approximately $x/C = -0.36$ to $x/C = -0.28$.

The flow over the aerofoil profile without the cavity was simulated using the computer code XFOIL [4], which is a panel code with coupled integral boundary layer solver. The code predicted a region of mildly separated flow along the tapered tail section of the pressure side of the aerofoil, with separation suggested at $x/C = -0.30$, consistent with the flow visualisation.

Discussion

The strong velocity fluctuation and high coherence found at the cavity trailing edge suggests that a highly receptive point is located there, while figure 9 shows that the convective disturbance is initiated near the same point. This supports the notion of an aeroacoustic feedback loop between the aerofoil trailing edge, where tonal noise is thought to be generated by diffraction of the shear layer disturbances, and the cavity trailing edge, where this noise 'drives' further boundary layer disturbances. Figure 12 shows a sketch of the overall tonal noise mechanism.

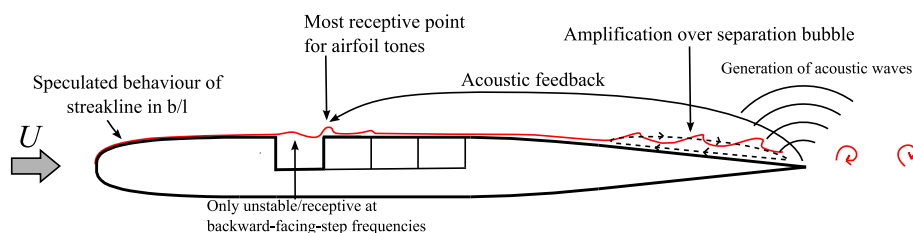


Figure 12. Sketch of proposed tonal noise mechanism for the streamlined plate with cavity.

Nash *et al.* [8] stated that a region of separation near the trailing edge is important for amplifying the instabilities. Referring to figure 7, strong growth of the disturbance indeed occurs downstream of around $x/C = -0.35$, where the flow is believed to be mildly separated. However they refuted the necessity of an aeroacoustic feedback loop of the form suggested by Arbey and Bataille [1], while in this instance such a loop appears to *also* be involved in the production of the tones.

Conclusions

The production of aerofoil tones has been found from flow over a streamlined plate with cavity. In this instance, both an aeroacoustic feedback loop *and* a region of separation approaching the trailing edge are believed to play a role in the production of the tones.

References

- [1] Arbey, H and Bataille, J, 1983, 'Noise generated by airfoil profiles in a uniform laminar flow', *J. Fluid Mech.*, vol. 134 pp. 33-47.
- [2] Arcondoulis, E J G, Doolan, C J, Zander, A C, and Brooks, L A, 2010, 'A review of trailing edge noise generated by airfoils at low to moderate Reynolds number', *Acoustics Australia*, vol. 38 no. 3 pp. 129-133.
- [3] Brooks, T F, Pope, D S, and Marcolini, M A, 1989, 'Airfoil self-noise and prediction', NASA Tech. Rep. 1218.
- [4] Drela, M, 1989, 'XFOIL: An Analysis and Design System for Low Reynolds Number Airfoils', *Springer-Verlag Lec. Notes in Eng.*, vol. 54.
- [5] Ikeda, T, Atobe, T, and Takagi, S, 2012, 'Direct simulations of trailing-edge noise generation from two-dimensional airfoils at low Reynolds numbers', *J. Sound Vib.*, vol. 331 pp. 556-574.
- [6] Jones, L E, and Sandberg, R D, 2011, 'Numerical analysis of tonal airfoil self-noise and acoustic feedback-loops', *J. Sound Vib.*, vol. 330 pp. 6137-6152.
- [7] Milbank, J, Watkins, S, and Kelso, R, 2001, 'An Instance of Cavity Resonance Interaction with an Open-Jet Tunnel Free Shear Layer', *Proceedings of the 14th Australasian Fluid Mechanics Conference*.
- [8] Moreau, D J, Brooks, L A, and Doolan, C J, 2011, 'On the aeroacoustic tonal noise generation mechanism of a sharp edged plate', *J. Acoust. Soc. Am.*, vol. 129 no. 4 pp. EL154-EL160.
- [9] Nash, E C, Lawson, M V, and McAlpine, A, 1999, 'Boundary-layer instability noise on airfoils', *J. Fluid Mech.*, vol. 382 pp. 27-61.
- [10] Paterson, R W, Vogt, P G, Fink, M R, and Munch, C L, 1973, 'Vortex noise of isolated airfoils', *J. Aircraft*, vol. 10 no. 5 pp. 296-302.
- [11] Sarohia, V. 1977, 'Experimental Investigation of Oscillations in Flows Over Shallow Cavities', *AIAA Journal*, vol. 15 no. 7 pp. 984-991.
- [12] Takagi, S, and Konishi, Y, 2010, 'Frequency Selection Mechanism of Airfoil Trailing-Edge Noise', *J. Aircraft*, vol. 47 pp. 1111-1116.